High-Pressure Laminar Flame Speed Measurements of an Ammonia/Hydrogen/Nitrogen Fuel Blend

Upom L. Costa, Yousef M. Almarzooq, Adi Hardaya, Matthew K. Hay, Waruna D. Kulatilaka, Eric L. Petersen
J. Mike Walker '66 Department of Mechanical Engineering, Texas A&M University
College Station, Texas 77843, USA

1 Introduction

Partially cracked NH_3 combustion research has focused on optimizing the cracking percentage to create a drop-in fuel replacement for CH_4-air combustors [1, 2]. Jiang et al. [2] conducted a numerical study at gas-turbine relevant conditions and found that mixtures with α = 60% had similar adiabatic flame temperatures and laminar flame velocities to CH_4-air combustion [1, 2]. Note that α is the cracking percentage shown in Eqn. 1. Partial cracking can be controlled by heating pure NH_3 gas to achieve the desired blend. Wiseman et al. [3] also found that the α = 60% blend had increased blow-out velocities and higher heat release rates compared to CH_4-air flames. According to Eqn. 1, an α = 60% mixture corresponds to 40% NH_3, 45% H_2, and 15% N_2 and will be referred to as the $0.4NH_3$+$0.45H_2$+$0.15N_2$ blend. This blend has the potential to be a drop-in fuel for many CH_4 combustors and has been studied numerically and experimentally [4, 5]. Before widespread use of this fuel is feasible, a better understanding of the fundamental reaction mechanisms of partially cracked NH_3 combustion is required.

$$NH_3 \rightarrow (1-\alpha)NH_3 + \alpha(0.75H_2 + 0.25N_2) \quad (1)$$

This paper presents new experimental laminar flame speed data for the target fuel blend over a range of pressures and using two types of experimental apparatus and associated diagnostics—a spherical flame and a high-pressure Bunsen flame. A summary of the two different experiments and related methodology is provided, followed by the new measurements. The results are analyzed and are compared against the predictions of current chemical kinetics models.

2 Experimental Method

2.1 Spherical Flame Measurement Apparatus: This study utilized the turbulent flame speed vessel (TFSV) located at the TEES Turbomachinery Laboratory of Texas A&M University (TAMU). The vessel, cylindrical in design, features an internal diameter of 35.6 cm, a length of 40.7 cm, and a total volume of 33.8 L. For optical diagnostics, the vessel is equipped with four opposing transparent windows, each with a diameter of 12.7 cm (5 in.) (Figure 1a).

The filling and venting processes during the experiments were managed using remotely operated pneumatic valves, ensuring precise control and improved sealing with the assistance of needle valves. The partial pressure method was employed to sequentially fill the vessel with the desired gases. At leaner conditions, flame fronts exhibited instabilities and cellular structures. A helium-oxygen mixture was used as the oxidizer to prevent this instability at higher pressures (3 and 4 atm). Homogeneous mixing of the gas mixture was ensured by operating a fan mounted on the vessel for 30 seconds prior to ignition. Ignition was initiated remotely from a control room using a system comprising a 10-μF capacitor, an automotive coil, a solenoid switch, and an adjustable, constant-current power supply. The spark ignition system, consisting of an alloy X electrode and ground rod, facilitated reliable ignition of the gas mixture.

A Z-type schlieren imaging system was employed to capture spherically propagating flames. A high-speed camera (Photron Fastcam SA1.1) operating at 7500 frames per second was used for image

Correspondence to: upomlcosta@tamu.edu

acquisition (Figure 1b) Light from a mercury arc lamp was collimated through a lens having a focal length of 800 mm. The collimated light was directed by two Figure 1 flat mirrors at 45° angles onto a knife edge, which removed excess light before entering the camera. Schlieren images were processed using an in-house edge-detection code. The stretch effects were corrected using non-linear equations from Chen [6]. Finally, unstretched, unburned laminar flame speed was calculated using the density ratio from equilibrium flame chemistry. Additional details can be found in [7-9].

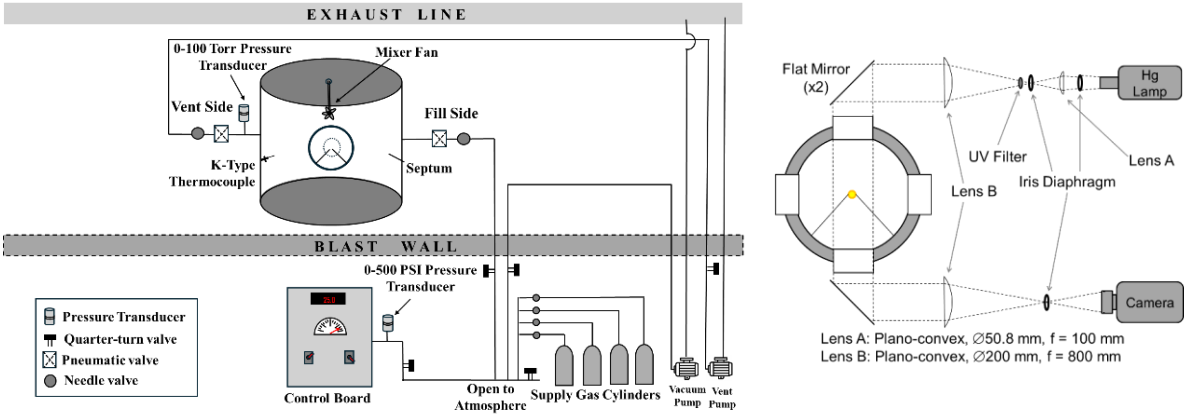

(a) (b)

Figure 1: (a) Experimental setup at TAMU for laminar flame speed measurements. (b) Optical setup for laminar flame speed experiments inside the TFSV vessel at TAMU.

2.2 Bunsen Burner Experimental Apparatus: The same $0.4NH_3+0.45H_2+0.15N_2$ flame was stabilized in an enclosed, 8.5-mm Bunsen burner to measure the flame speed. The central jet is surrounded by a 13.5-mm thick annular air co-flow ring used to help stabilize the flame. A N_2 guard flow surrounds the air co-flow to cool the enclosure and UVFS optical windows surrounding the burner. The enclosed burner was used to seal the burner from the operators, and the air co-flow and N_2 guard flow were kept to a minimum to maintain atmospheric pressure within the burner. The fuel blend and air were mixed well before the burner outlet to ensure complete mixing. The fuel flowrate was fixed for all flames at 1.10, 1.24, and 0.414 slm for NH_3, H_2, and N_2, respectively. The premixed air flowrate was varied between 5.31–8.12 slm for $\Phi = 0.85–1.3$. The air co-flow and N_2 guard flow rates were fixed at 6 and 8 slm. Gas flowrates were controlled by MKS and Bronkhorst mass flow controllers.

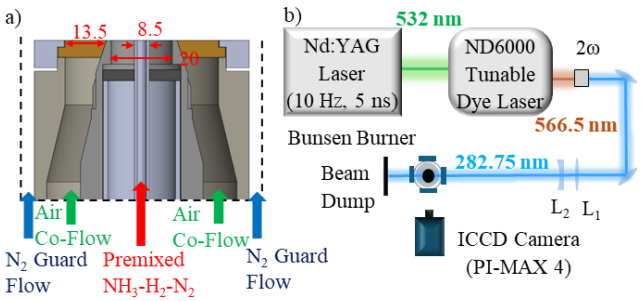

Figure 2:(a) Enclosed Bunsen burner schematic. Dimensions shown in mm. (b) OH PLIF experimental apparatus schematic including an Nd:YAG laser, tunable dye laser, frequency doubling crystal, f = + 750 mm plano convex lens (L1), f = - 75 mm cylindrical lens (L2), and ICCD camera

OH planar laser-induced fluorescence (PLIF) was used to illuminate the reaction zone of the Bunsen flame. A ns-duration, pulsed Nd:YAG laser (Continuum, Model: Powerlite 8000) was frequency doubled to generate 532-nm pulses, which then pumped a tunable dye laser (Continuum, Model: ND 6000) circulating a solution of Rhodamine-590 dye mixed in methanol to generate 565.500-nm laser pulses. These laser pulses were frequency doubled in a beta-barium borate (BBO) crystal to generate

282.750-nm laser pulses. A Highfinesse wavemeter monitored the output of the dye laser to ensure the proper wavelength to excite the OH Q1(5) transition line. The 282.750-nm laser pulses were directed to the probe volume by four 45° dielectric mirrors. A f = 750 mm plano-convex lens and a f = -75 mm cylindrical lens were used to produce a ~ 25-mm tall laser sheet that was focused in the center of the Bunsen burner. The laser energy was maintained at 40 mJ/pulse for all OH-PLIF measurements. OH fluorescence was collected by a UV-optimized intensified charge-coupled device (ICCD) camera (Princeton Instruments, Model: PI-Max4) and a f = 100 mm f/2 UV camera lens (Bernad Halle). An optical bandpass filter centered at 315 nm with a 15 nm FWHM bandwidth (Semrock FF01-315/15-50) was placed in front of the camera lens to spectrally isolate the OH LIF signal. The camera was placed orthogonally to the direction of beam propagation (Figure 2).

3 Results and Discussion

3.1 Spherical Flame Results: The experimentally measured laminar flame speeds at 1 atm were compared with predictions from four different chemical kinetics models, revealing significant variations among the models (Figure 3). The highest peak flame speed, 46.5 cm/s, was predicted by the Stagni et al. model [10], while the Okafor et al. model [11] predicted a lower peak value of 31.5 cm/s. The experimental peak flame speed was observed at 42 cm/s. Across all equivalence ratios, the Okafor et al. model [11] underpredicted flame speeds by 10–15 cm/s compared to Stagni et al [10]. Notably, the experimental results showed good agreement with the KAUST mechanism [12], with maximum deviations of 5 cm/s on the lean and rich sides. The practical flammability range was found to be between $\Phi \sim 0.8$ and $\Phi \sim 1.4$.

Additionally, two experimental results having similar blends from the literature were compared. The mixture studied by Mei et al. [13], which incorporated 40% cracked NH_3, yielded values closely aligned with the findings of this study. In contrast, Ji et al. [1], who tested the same mixture composition as this study at 303 K (5 K higher) and 0.1 MPa, reported significantly higher peak laminar flame speeds, around 50 cm/s. A similar trend was observed at elevated pressures, where the Stagni et al. model [10] overpredicted the experimental laminar flame speeds, while the Okafor et al. model [11] underpredicted them. At 2 atm, the experimental data showed the best agreement with the KAUST mechanism [12], with a peak laminar flame speed of approximately 34 cm/s (Figure 3). The practical flammability range was constrained between equivalence ratios of 0.9 and 1.35.

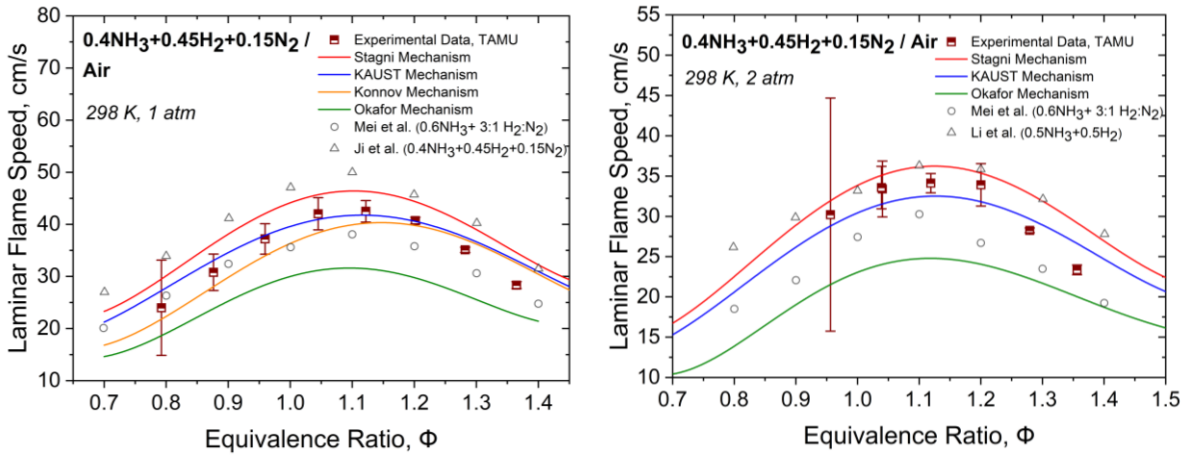

Figure 3: Laminar Flame Speeds of $0.4NH_3+0.45H_2+0.15N_2$ / Air at 298 K, 1 atm (left) and 2 atm (right).

The uncertainties associated with these plots warrant careful consideration. Stretch effects were corrected by ignoring unusable datapoints from a dr/dt-versus-stretch plot while accounting for any instability, ignition, or potential end-wall effects. For an unstable flame, an acceleration is noticed past a certain radius suggesting transition to turbulence (Figure 4b). Both instability and ignition effects were

observed from the higher deviations in flame speeds in Figure 4b. Affected frames were excluded from the analysis to ensure accurate evaluation of laminar flame properties. NH_3/H_2 mixtures are known to exhibit cellular instability at lean equivalence ratios. At 1 and 2 atm, lean equivalence ratios showed an increased propensity for instability (Figure 4a), resulting in even fewer data points being available for calculation of the laminar flame speed (Figure 4b). Consequently, this narrow region of usable data led to larger uncertainty intervals, particularly at $\Phi = 0.8$ and 0.9. Conversely, these disturbances were not observed on the rich side, where the expanding flame front remained predominantly spherical (Figure 4a), yielding consistent results.

To address this instability issue, for pressures exceeding 2 atm, the oxidizer mixture was adjusted by substituting all N_2 with He. Equilibrium thermochemistry analysis was conducted using Chemkin Pro to determine the optimal O_2:He ratio while maintaining the same adiabatic flame temperature as the original mixture. At 3 and 4 atm, it was revealed that a 1:6 oxygen-to-helium ratio was the most effective.

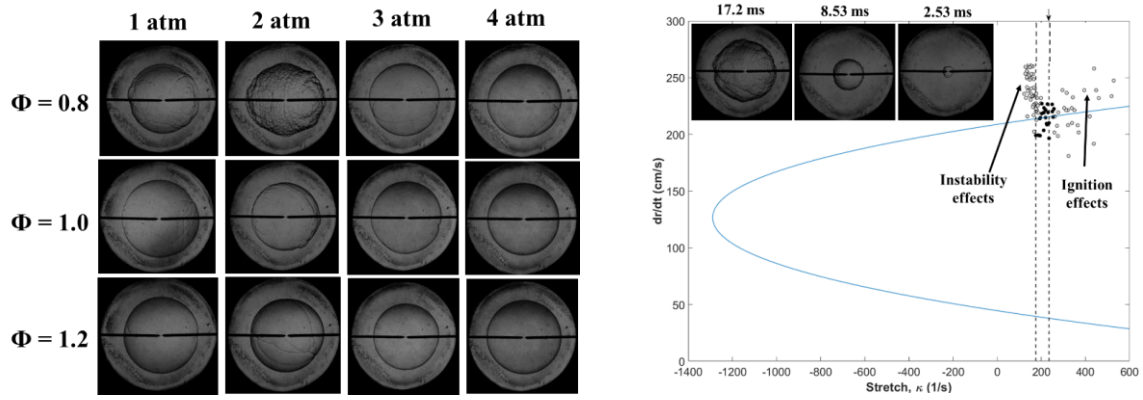

Figure 4: (a) Flame images at different equivalence ratios (Top to bottom: $\Phi = 0.8$, 1.0, and 1.2) and pressures (1 through 4 atm from left to right). (b) Burned gas velocity versus stretch for $\Phi = 0.95$ at 2 atm.

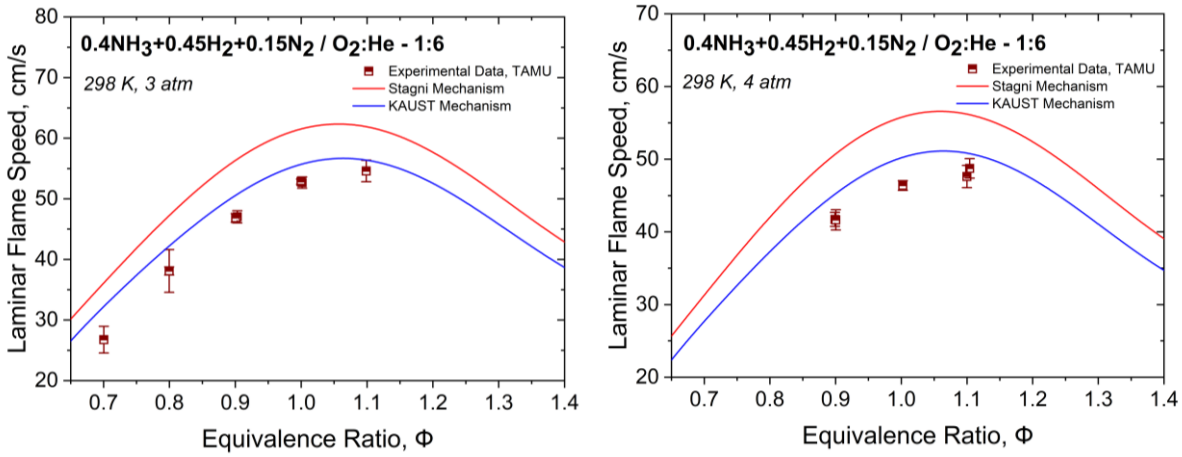

Figure 5: Laminar Flame Speeds of $0.4NH_3+0.45H_2+0.15N_2$ / O_2 : He – 1:6 at 298 K, 3 and 4 atm.

At 3 and 4 atm, the results for leaner mixtures showed significant improvement, with reduced uncertainty intervals and closer alignment with kinetics model predictions (Figure 5). The peak laminar flame speed was approximately 54.6 cm/s at 3 atm and 48 cm/s at 4 atm. The addition of He notably improved flame shape uniformity (Figure 4a) and extended the flammability range on the lean side. However, mixtures with equivalence ratios exceeding 1.2 failed to ignite using the current setup. The KAUST mechanism [12] slightly overpredicted flame speeds for helium-oxygen mixtures at both pressures (Figure 5). Replacing nitrogen with helium enhanced overall flame speeds by 50%, even at elevated pressures. Between 1 and 2 atm, flame speeds decreased by 20%, while the reduction between

3 and 4 atm was around 10%. Across all pressure conditions, the KAUST mechanism [12] provided the closest agreement with the experimental data.

3.2 Bunsen Flame Results: The steep OH gradient at the flame front makes OH-PLIF a useful tool for imagining the entire Bunsen flame cone. After the flame cone is clearly identified, the half-angle and known gas velocity can be used to measure the laminar flame speed. Hu et al. [14] used this approach to compare the experimental laminar flame speed and 2D simulations. In this work, a Canny edge detection algorithm identified the flame front from the recorded background subtracted OH-PLIF images. A linear fit was used to fit the flame front, and the half-cone angle was measured from the linear fit. The curvature at the base of the flame and the tip of the flame caused errors in the linear; therefore, they were not considered in this analysis. The flame speed was corrected for stretch effects following the discussion by Hu et al. [14]. This correction requires the local strain rate (K_s), local curvature (κ), and local uncorrected laminar flame speed at the same radial location along the flame front. This method required a 2nd-degree polynomial fit along the flame front.

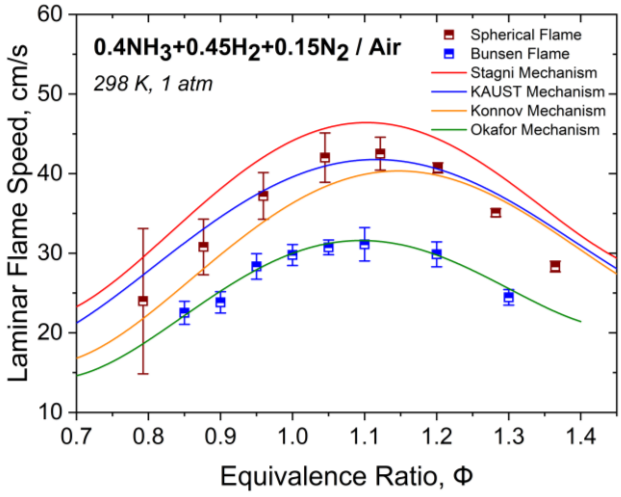

Figure 6: Spherical and Bunsen flame results comparison at 298 K and 1 atm

The average flame speed, S_d was calculated from multiple points along the middle 80% of the flame and are shown in Figure 6b. The error bars represent ± 2σ of 50 averaged flame speed measurements. Flame speed measurements at 1 atm in the Bunsen burner are compared to 1-atm flame speed measurements shown in the earlier section along with several model predictions in Figure 6b. The Bunsen burner flame is ~ 10 cm/s slower than the spherical flame. Interestingly, these results align closely with predictions from the Okafor mechanism [11]. In 2010, C.K. Law [15] highlighted that in flat-flame burners, flame stabilization is achieved through heat transfer to the burner surface, which makes the flame non-adiabatic relative to the free-stream enthalpy. As a result, the flame speed determined in this process might be lower in comparison to LFS based on free stream properties. Further investigation is required to understand why Bunsen flame speed measurements are slower and why they align better with the Okafor mechanism [11], which otherwise showed poor agreement with the spherical flame data. These findings highlight a potential source of discrepancies in kinetics model predictions and underscore the need for careful consideration when comparing results across different experimental setups.

4 Conclusions

Laminar flame speeds were measured at 298 K across four pressures (1–4 atm) and were compared with predictions from four chemical kinetics models. Differences between Bunsen flames and spherically expanding flames at 1 atm were highlighted. At 1 and 2 atm, air was used as the oxidizer. Peak laminar flame speeds were 42 and 34 cm/s, respectively, at Φ = 1.1. Leaner equivalence ratios showed

instabilities at the flame front resulting in higher uncertainties. At 3 and 4 atm, to promote stability, 1:6 O_2:He mixture was used as the oxidizer. This modified oxidizer resulted in significant improvement on lean-side flame measurements. Peak laminar flame speeds increased to 54.6 cm/s at 3 atm and 48 cm/s at 4 atm, both at ϕ=1.1. Replacing nitrogen with helium increased flame speeds by 50%. Otherwise, the predicted trend of decreasing laminar flame speeds with increasing pressures was observed. Across all conditions, the Stagni-PoliMi mechanism consistently overpredicted laminar flame speeds, while the KAUST mechanism demonstrated the best agreement with experimental data. Bunsen flame speeds were compared with spherically expanding flame results at 1 atm. Bunsen flames were 10 cm/s slower at all equivalence ratios. Okafor mechanism showed better agreement with Bunsen flame results. These findings provide valuable insights into the effects of pressure, oxidizer composition, and flame geometry on laminar flame speeds, contributing to the refinement of ammonia-based combustion models and their application in high-pressure environments.

References

[1] Ji C, Wang Z, Wang D, Hou R, Zhang T, Wang S. (2022). Experimental and numerical study on premixed partially dissociated ammonia mixtures. Part I: Laminar burning velocity of NH3/H2/N2/air mixtures. International Journal of Hydrogen Energy.47(6):4171-84.
[2] Jiang Y, Gruber A, Seshadri K, Williams F. (2020). An updated short chemical-kinetic nitrogen mechanism for carbon-free combustion applications. International Journal of Energy Research.44(2):795-810.
[3] Wiseman S, Rieth M, Gruber A, Dawson JR, Chen JH. (2021). A comparison of the blow-out behavior of turbulent premixed ammonia/hydrogen/nitrogen-air and methane–air flames. Proceedings of the Combustion Institute.38(2):2869-76.
[4] Hardaya AP, Hay MK, S. Soriano B, Chen J, Kulatilaka WD. (2024). NH Imaging in Premixed Ammonia/Hydrogen Flames Using Femtosecond Laser-Induced Fluorescence. AIAA SCITECH 2024 Forum2020.
[5] Hardaya AP, Kulatilaka WD, Soriano BS, Chen JH. (2024). Heat release surrogates for NH3/H2/N2–air premixed flames. Proceedings of the Combustion Institute.40(1-4):105432.
[6] Chen Z. (2011). On the extraction of laminar flame speed and Markstein length from outwardly propagating spherical flames. Combustion and Flame.158(2):291-300.
[7] Lowry W, de Vries J, Krejci M, Petersen E, Serinyel Z, Metcalfe W, et al. (2011). Laminar Flame Speed Measurements and Modeling of Pure Alkanes and Alkane Blends at Elevated Pressures. Journal of Engineering for Gas Turbines and Power.133(9).
[8] Morones A, Turner MA, León V, Ruehle K, Petersen EL, editors. Validation of a New Turbulent Flame Speed Facility for the Study of Gas Turbine Fuel Blends at Elevated Pressure. ASME Turbo Expo 2019: Turbomachinery Technical Conference and Exposition; 2019. V04AT04A024.
[9] Sikes T, Mannan MS, Petersen EL. (2018). An experimental study: laminar flame speed sensitivity from spherical flames in stoichiometric CH4–air mixtures. Combustion Science and Technology.190(9):1594-613.
[10] Stagni A, Cavallotti C, Arunthanayothin S, Song Y, Herbinet O, Battin-Leclerc F, Faravelli T. (2020). An experimental, theoretical and kinetic-modeling study of the gas-phase oxidation of ammonia. Reaction Chemistry & Engineering.5(4):696-711.
[11] Okafor EC, Naito Y, Colson S, Ichikawa A, Kudo T, Hayakawa A, Kobayashi H. (2019). Measurement and modelling of the laminar burning velocity of methane-ammonia-air flames at high pressures using a reduced reaction mechanism. Combustion and Flame.204:162-75.
[12] Zhang X, Moosakutty SP, Rajan RP, Younes M, Sarathy SM. (2021). Combustion chemistry of ammonia/hydrogen mixtures: Jet-stirred reactor measurements and comprehensive kinetic modeling. Combustion and Flame.234:111653.
[13] Mei B, Zhang J, Shi X, Xi Z, Li Y. (2021). Enhancement of ammonia combustion with partial fuel cracking strategy: Laminar flame propagation and kinetic modeling investigation of NH3/H2/N2/air mixtures up to 10 atm. Combustion and flame.231:111472.
[14] Hu S, Gao J, Gong C, Zhou Y, Bai dX, Li Z, Alden M. (2018). Assessment of uncertainties of laminar flame speed of premixed flames as determined using a Bunsen burner at varying pressures. Applied energy.227:149-58.
[15] Law CK. (2010). Combustion Physics: Cambridge University Press.